

Cyclic Properties of Superelastic Shape Memory Alloy Wires and Bars

Reginald DesRoches, M.ASCE¹; Jason McCormick²; and Michael Delemont³

Abstract: This study evaluates the properties of superelastic Ni–Ti shape memory alloys under cyclic loading to assess their potential for applications in seismic resistant design and retrofit. Shape memory alloy wire and bars are tested to evaluate the effect of bar size and loading history on the strength, equivalent damping, and recentering properties of the shape memory alloys in superelastic form. The bars are tested under both quasistatic and dynamic loading. The results show that nearly ideal superelastic properties can be obtained in both wire and bar form of the superelastic Ni–Ti shape memory alloys. However, the wire form of the shape memory alloys show higher strength and damping properties compared with the bars. The recentering capabilities (based on residual strains) are not affected by section size. Overall, the damping potential of shape memory alloys in superelastic form is low for both wire and bars, typically less than 7% equivalent viscous damping. Cyclical strains greater than 6% lead to degradation in the damping and recentering properties of the shape memory alloys. Strain rate effects are evaluated by subjecting the shape memory alloys to loading rates representative of typical seismic loading. The results show that increased loading rates lead to decreases in the equivalent damping, but have negligible effects on the recentering properties of the shape memory alloys.

DOI: 10.1061/(ASCE)0733-9445(2004)130:1(38)

CE Database subject headings: Seismic properties; Cyclic tests; Damping; Strain rate; Shape memory effect.

Introduction

Shape memory alloys are unique alloys that have the ability to undergo large deformations, but can return to their undeformed shape by heating (known as the shape memory effect) or through removal of the stress (known as the superelastic effect). Although first discovered in the 1960s, shape memory alloys (SMAs) have found functional applications only in the past 15–20 years. The high cost, lack of clear understanding of the thermo-mechanical processing, and the inability to reliably predict the behavior of shape memory alloys were the reasons for the slow introduction of the material into application. Higher quality and reliability, coupled with a significant reduction in price has recently led to numerous applications of shape memory alloys in the biomedical, commercial, and aerospace industries.

Driven by a search for devices that could result in less invasive medical procedures, researchers have found numerous applications for shape memory alloys in the medical field. Arterial stents, medical guidewires, catheters, orthodontic braces, and orthopedic prostheses have all taken advantage of the unique properties of superelastic shape memory alloys (Duerig et al. 1990). In the aerospace industry, shape memory alloys have been used in adaptive aircraft wings and smart helicopter blades for increased effi-

ciency and reduced noise and vibration (Beauchamp 1992; Chandra 2001). Recent years have seen numerous commercial and consumer applications of shape memory alloys. Eye glass frames, cellular telephone antennas, frames for brassiers, and golf clubs all take advantage of the superelastic properties of SMAs (Asai and Suzuk 2000; Hsu et al. 2000).

Recently, there has been increasing interest in using superelastic shape memory alloys for applications in seismic resistant design of structures. Grasser and Cozzarelli (1991) suggested the use of binary nickel–titanium shape memory alloys (Nitinol) as seismic dampers. Binary nickel–titanium shape memory alloys are commonly referred to as Nitinol (Nickel Titanium Naval Ordnance Laboratory). They studied the effect of loading frequency and history on the energy dissipation characteristics of Nitinol wires. They also proposed a one-dimensional constitutive model for the superelastic behavior and verified the model with experimental work. Using a unidirectional shaking table, Inaudi and Kelly (1994) studied a four-story steel-frame model with tuned mass dampers using shape memory alloy wires. The number of SMA wires and the prestress tension were varied to study their effect on the building response. The study found that significant improvement was obtained in the dynamic response of the structure when the prestress tension was tuned to the first natural frequency of the isolated structure. Sweeney and Hayes (1995) and Clarke et al. (1995) found that SMA wires can reduce displacements and accelerations in structures, although the extent of reduction varied between the different studies. Recently, researchers in Japan have been investigating the use of SMA dampers on bridges (Adachi and Unjoh 1999; Wilde et al. 2000). Both studies showed that bridge deck displacements can be reduced with the use of SMA dampers. Several studies have investigated the use of SMA elements in seismic rehabilitation of steel frame buildings. Ohi (2001) tested superelastic bracing elements using ternary NiTiCo SMAs. The braces were found to return to their original shapes after being subjected to strains as large as 5%. Also, the

¹Assistant Professor, Georgia Institute of Technology, Atlanta, GA 30332-0355. E-mail: reginald.desroches@ce.gatech.edu

²PhD Candidate, Georgia Institute of Technology, Atlanta, GA 30318.

³URS. Corp., Rolling Meadows, IL 60008.

Note. Associate Editor: Gregory A. MacRae. Discussion open until June 1, 2004. Separate discussions must be submitted for individual papers. To extend the closing date by one month, a written request must be filed with the ASCE Managing Editor. The manuscript for this paper was submitted for review and possible publication on September 4, 2002; approved on March 26, 2003. This paper is part of the *Journal of Structural Engineering*, Vol. 130, No. 1, January 1, 2004. ©ASCE, ISSN 0733-9445/2004/1-38–46/\$18.00.

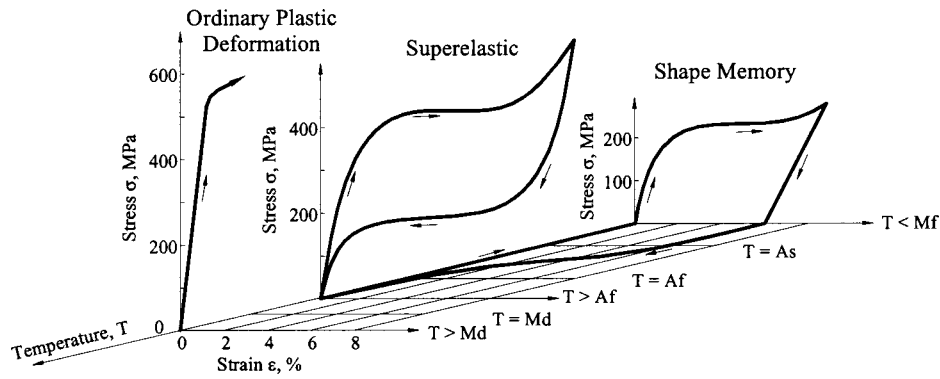


Fig. 1. Three-dimensional stress–strain temperature diagram showing deformation and shape memory behavior of NiTi shape memory alloy

bracing provided some moderate damping for strains greater than 1%. Ocel et al. (2002) investigated beam–column connections using 35 mm diameter martensitic SMA rods. The SMA connection was found to exhibit a stable and repeatable hysteresis for cyclic loads up to 4% story drift. After the initial tests, the SMA rods were heated above their transformation temperature and were able to recover approximately 76% of their residual deformation. The most substantial effort thus far in the area of seismic applications of SMA has been from the Memory Alloys for New Seismic Isolation and Energy Dissipation Devices (MANSIDE) Project. This project was a multiyear effort by the European Union to evaluate the efficacy of the shape memory alloys in seismic isolation (MANSIDE 1998). The project included both experimental studies and analytical modeling and resulted in a much better understanding of the behavior of SMA wires under tension loads, and SMA bars under torsion loads (Dolce and Marretto 1999; Dolce and Cardone 2001a, 2001b). The results of the project show there is promise for shape memory alloys in seismic isolation. However, significant research is still needed, particularly as it pertains to large section properties. Most of the studies above used shape memory alloy wires or thin bars. There is currently little available data on the performance of large diameter shape memory alloy bars, and anecdotal evidence has suggested that superelastic properties are difficult to achieve for large diameter shape memory alloy bars.

This paper presents the results of a study evaluating the characteristics of shape memory alloy wire and bars to determine the effects of bar size, loading history, and loading rate on the cyclic properties of shape memory alloys. The properties that are evaluated are those which are most important for seismic applications such as energy dissipation, recentering capabilities, and transformation stresses. Recentering refers to the ability of the material to return to its original undeformed shape upon unloading. The SMA wires and bars used in this study are superelastic and are composed of the binary nickel–titanium alloy.

Shape Memory Alloys

Shape memory alloys are materials that have the unique ability to recover their shape after undergoing large deformations through either heating (known as shape memory effect) or removal of load (known as the superelastic effect). The unique property is made possible by a martensitic phase transformation between a crystallographic high-symmetry (cubic crystal structure) austenitic phase to a low-symmetry (monoclinic crystal structure) martensitic phase. Typically, martensite is stable at low temperatures and high

stress values, whereas austenite is stable at high temperatures and low stress values. The mechanical behavior as a function of temperature, strain, and stress is summarized in Fig. 1. Below the martensite finish temperature, M_f , the SMA exhibits the shape memory effect. Deformations due to an applied stress are recovered by heating the material above the austenite finish temperature, A_f . At a temperature above A_f , the SMA is in its parent phase, austenite. Upon loading, stress-induced martensite is formed. Upon unloading, however, the material reverts to austenite at a lower stress, thereby resulting in the superelastic behavior. The resulting nonlinear stress–strain relationship results in a hysteresis. In the context of this paper, hysteresis refers to the nonsingle-valued stress–strain relationships for the NiTi SMA. At a yet higher temperature (above M_d), the SMA undergoes ordinary plastic deformation with much higher strength.

Superelastic shape memory alloys possess several characteristics that make them desirable for applications in seismic resistant design and retrofit in structures. These characteristics include: (1) hysteretic damping; (2) large elastic strain range, resulting in recentering capabilities; (3) excellent low- and high-cycle fatigue properties; (4) strain hardening at large strains; and (5) a stress plateau, providing force transmission limitations. Table 1 shows a summary of the mechanical properties of NiTi shape memory alloys.

Experimental Tests of Superelastic Wires and Bars

As mentioned in the above section, the superelastic properties of shape memory alloys may be ideally suited for applications in

Table 1. Properties of NiTi Shape Memory Alloys

Property	NiTi SMA	
	Austenite	Martensite
Physical properties		
Density	6.45 g/cm ³	
Mechanical properties		
Recoverable elongation	up to 8%	
Young's modulus	30–83 GPa	21–41 GPa
Yield strength	195–690 MPa	70–140 MPa
Ultimate tensile strength	895–1,900 MPa	
Elongation at failure	5–50% (typically 25%)	
Poisson's ratio	0.33	
Chemical properties		
Corrosion performance	Excellent (similar to stainless steel)	

Table 2. Shape Memory Alloy Test Specimen

Set	Diameter (mm)	Specimen length (mm)	Gage length (mm)	A_s (°C)	Weight (%)		Processing	Cold work	Annealing temperature (°C)
					Ni	Ti			
1	1.8	152	63.5	-26	56.05	43.95	Cold drawn	30%	350
2	7.1	152	57	-10	56.00	44.00	Hot rolled	None	350
3	12.7	152	57	-10	55.90	44.10	Cold drawn	30%	350
4	25.4	279.4	152	-11	56.00	44.00	Cold drawn	25%	450

seismic resistant design and retrofit. While there have been numerous studies on the properties of superelastic shape memory alloys (Kawaguchi et al. 1991), few of these studies have been under cyclic loading histories and rates expected during earthquakes. In addition, the properties that have been characterized are typically different from those that are important for seismic applications. Moreover, few of these have been performed for bar sizes that might be used in civil engineering applications.

In this study, SMA wires and bars up to 25.4 mm (1.0 in.) in diameter are tested to determine their mechanical characteristics. The tests are performed under cyclic tension loading up to 6% strain under both quasistatic and dynamic loading. The mechanical properties that are evaluated include the residual strains (ϵ_r), forward and reverse transformation stresses (σ_L , and σ_{UL}), and energy dissipation (ξ_{eq}). Residual strain refers to the remaining strain at the end of a cycle when the specimen returns to a state of zero stress. The transformation stress is not straight forward to identify because of changes in the shape of the hysteresis loop represented by the nonlinear cyclic stress-strain plot. For the purpose of this paper, the forward transformation stress is evaluated as the stress at 2% strain. For this reason, no value for σ_L is reported for the first two cycles. The reverse transformation stress is much more difficult to evaluate. It was obtained by estimating the inflection point along the unloading curve. Equivalent viscous damping is used as a measure of the energy dissipation during cycling and is defined the energy dissipated per cycle (area under force-deformation curve) divided by the product of 4π and the strain energy for a complete cycle.

Test Specimens and Loading Protocol

A number of specimens of each size, ranging from 1.8 mm (0.071 in.) diameter wires to 25.4 mm (1.0 in.) diameter bars were tested in this study. For each size, a number of samples ranging from six for the large bars to 10 for the smaller bars and wire were tested. Table 2 shows the size of the specimens, austenite start temperature, composition, and thermo-mechanical processing. All of the specimens had very low austenite start temperatures, and were superelastic at room temperature. The composition of all of the samples was nearly identical, with an average of 56.0% nickel by weight and 44.0% titanium. The 7.1 mm (0.28 in.) diameter bars were hot rolled, whereas the wires and larger diameter bars were cold drawn with 30% cold working, where the amount of cold working refers to the reduction in cross-sectional area of the specimen due to drawing. A larger percentage of cold working leads to increases in strength and hardness. Per recommendations from the manufacturer, the specimens were heat treated at 350°C (662°F) for 30 min, with the 25.4 mm (1.0 in.) diameter bars being heat treated at 450°C (842°F) for 1 h. All of the bars were water quenched.

The loading protocol used, shown in Fig. 2, consists of increasing strain cycles of 0.50%, 1.0–5% by increments of 1%, followed by four cycles at 6%. For the first series of tests, the

loading was performed at a frequency of 0.025 Hz, which corresponds to a maximum strain rate of approximately 0.3%/s. Subsequent testing was performed at loading frequencies of 0.5 and 1.0 Hz to simulate dynamic loading.

Experimental Setup

Testing of the 1.8 mm (0.071 in.), 7.1 mm (0.28 in.), and 12.7 mm (0.5 in.) diameter specimens was done using a 250 kN (55 kip) MTS hydraulic testing apparatus fitted with MTS 647 hydraulic wedge grips. Round specimen wedges were used to grip the bars with flat specimen wedges being used for the wire. The above mentioned loading protocol was input using an MTS TestStar Controller running *TestWare* software which used strain output from the extensometer to control the movement of the actuator. Strains were measured with a 25.4 mm (1.0 in.) gage length extensometer with the load being measured with the internal load cell of the actuator. Testing on the 25.4 mm (1.0 in.) diameter bar was performed using a 2.7 MN (600 kip) MTS uniaxial servo-controlled hydraulic frame and an INSTRON 8500 Plus controller. The ends of the 25.4 mm (1.0 in.) specimens were threaded to facilitate gripping of the specimens.

Cyclic Properties of Wires

Wires are the most common form of Nitinol SMA. While wires have been extensively tested, most tests have not evaluated the cyclic properties for loading histories that are similar to those found in seismic applications. The stress-strain curve for the 1.8 mm (0.071 in.) diameter wire, shown in Fig. 3, reveals several interesting pieces of information. First, the initial modulus of elasticity is approximately 40 GPa (5802 ksi). During early cycles, the forward transformation stress (henceforth referred to as the loading plateau stress, σ_L) occurred at approximately 550–

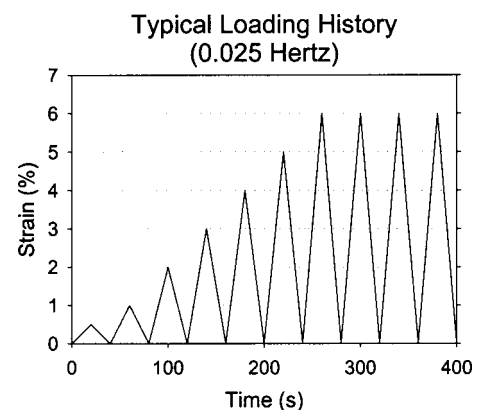


Fig. 2. Loading protocol for cyclic tests of shape memory alloy wires and bars

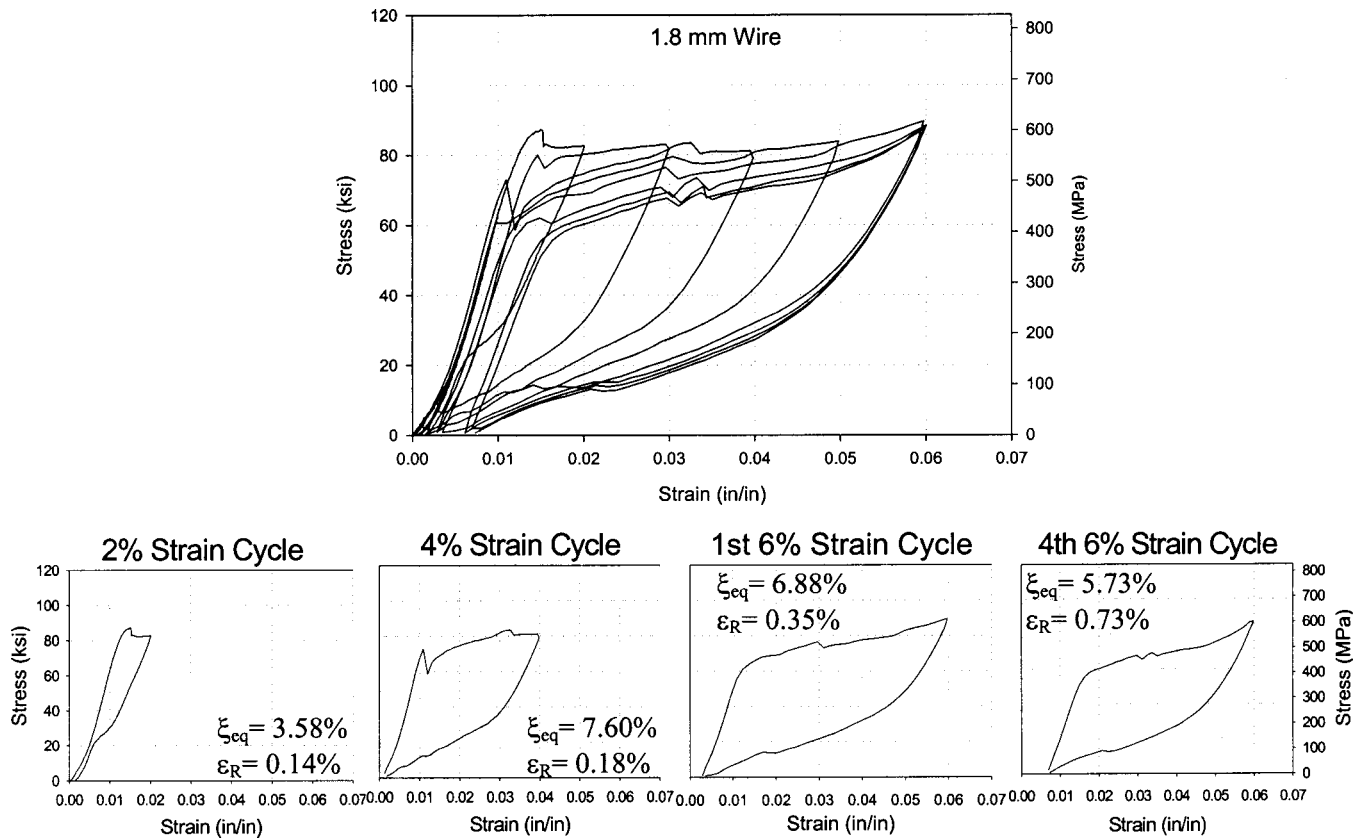


Fig. 3. Stress-strain behavior for 1.8 mm diameter nitinol shape memory alloy wire subjected to quasistatic cyclic loading

600 MPa (79.8–87.0 ksi). During later cycles, σ_L gradually decreased to approximately 400 MPa (58.0 ksi). The effect of decreasing loading plateau stresses with increasing cycles, commonly referred to as fatigue, have been previously studied for SMA wires. Fatigue, in the context of this study, refers to the degradation of properties (such as the reduction in σ_L) due to cyclic loading. The effect is considered to be associated with the introduction of small levels of localized slip that assist the forward transformation, which results in lower values of the forward transformation stress, σ_L (Miyazaki et al. 1986; Miyazaki 1990; Tobushi et al. 1992).

The reverse transformation stress (henceforth referred to as the unloading stress, σ_{UL}) occurs at approximately 200 MPa (29 ksi) for the 2% cycle to the first 6% cycle. Slight reductions are observed for the later 6% strain cycles. Previous studies have shown that the unloading plateau stress generally decreases less during cycling compared with decreases observed in the loading plateau stress (Strandl et al. 1995a; 1995b; Friend and Morgan 1999).

The residual strains after unloading increase after each cycle and range from 0.14% after the 2% strain cycle to 0.73% after the fourth 6% cycle. Previous studies have shown that the increase in residual strain with cycling is also due to small levels of localized slip and build-up of dislocations and will typically stabilize with increased cycling. Observe that the rate of increase in residual strain slows as the wires undergo the last two 6% cycles.

The equivalent viscous damping ratio, ξ_{eq} , for the wire is shown in Fig. 3 for each cycle. ξ_{eq} ranges from 3.58% for the 2% cycle to a maximum of 7.60% for the 4% strain cycle. The equivalent viscous damping slightly decreases for increasing 6% strain cycles. This results from the fact that σ_L is decreasing, while σ_{UL} essentially remains constant, resulting in smaller hys-

teresis. These results confirm previous studies on the properties of wire subjected to cyclical loading (Dolce and Cardone 2001b). Their study found that the maximum equivalent viscous damping occurred at around 5–6% strain and was in the range of $\xi_{eq} = 5-7\%$.

Cyclic Properties of 25.4 mm (1.0 in.) Bars

Since the majority of applications of superelastic shape memory alloys use them in the form of wires, there is little information on the behavior of large diameter shape memory alloy bars. The studies that were performed in the early 1990s found that SMA bars did not exhibit the superelastic properties that are found in wires. Even more recent studies from the MANSIDE project recommended using SMA wires instead of bars because of the enhanced performance of wires compared to bars (Dolce and Marretto 1999).

Fig. 4 shows the cyclical stress-strain diagram for a 25.4 mm (1.0 in.) diameter SMA bar, subjected to the same loading protocol as the wire discussed in the previous section. The initial modulus of elasticity, 28 GPa (4,061 ksi), and the loading plateau stress, 410 MPa (59.5 ksi), is approximately 30% less than the corresponding values for the wire. In later cycles, σ_L decreases to 375 MPa (54.4 ksi) due to the fatigue effect. The decrease in σ_L is considerably less than what was observed in the wires. This is most likely a result of the differences in thermo-mechanical treatment between the wires and the bars. Previous research has shown that thermo-mechanical processing has a significant effect on the superelastic cyclic stability of shape memory alloys (Friend and Morgan 1999). The reverse transformation stress, or unloading plateau, σ_{UL} , occurs at approximately 268 MPa (38.9

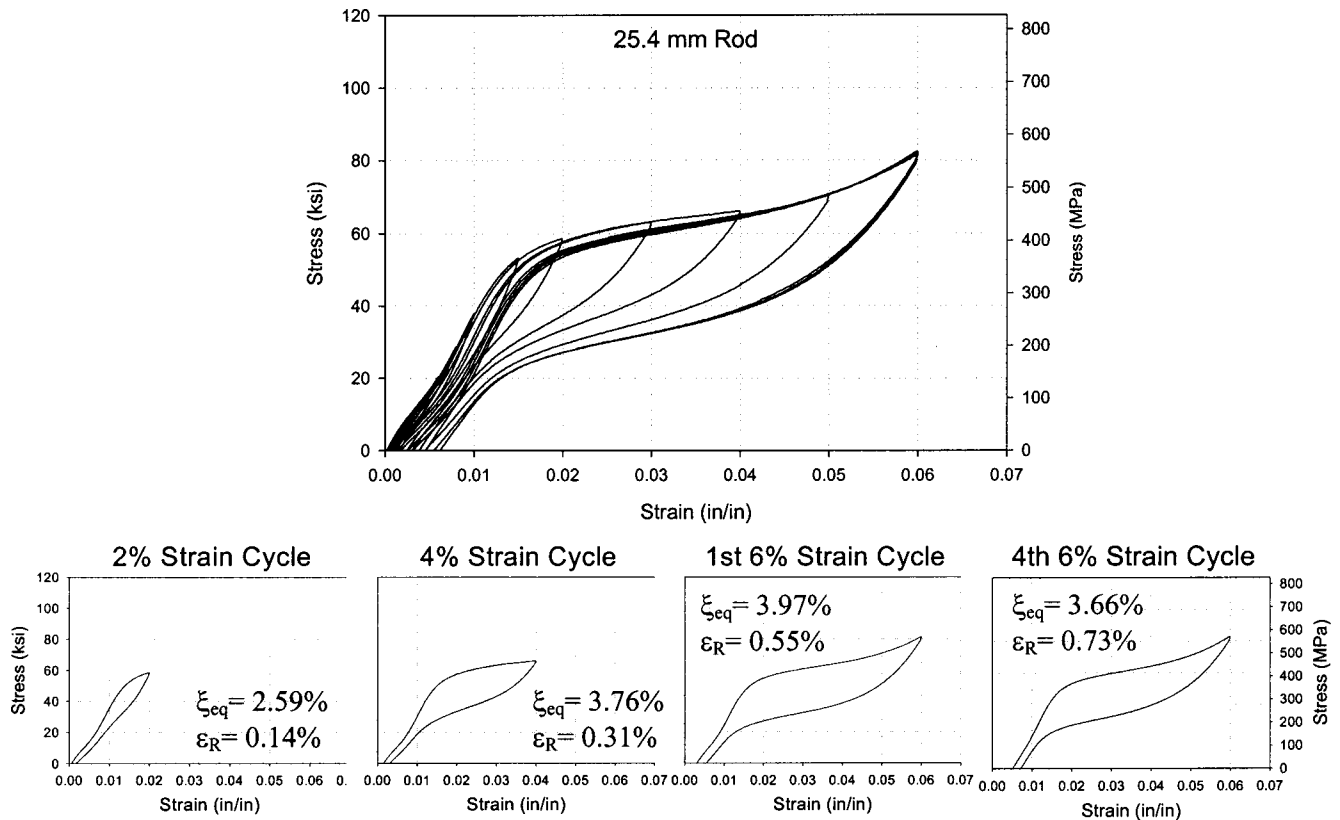


Fig. 4. Stress–strain for 25.4 mm diameter nitinol shape memory alloy bar subjected to quasistatic cyclic loading

ksi) for the 2% cycles and decreases to approximately 260 MPa (37.7 ksi) during the 6% cycles.

The residual strains in the SMA bar increase from 0.14% after 2% strain to 0.73% after the fourth 6% cycle. It appears that the residual strain begins to stabilize since the residual strain for the last three cycles at 6% strain are approximately the same. However, the residual strains in the bar are still very low, considering the bar was subjected to four cycles at 6% strain.

The equivalent viscous damping ratio, ξ_{eq} , for various cycles of the bar is shown in Fig. 4. ξ_{eq} ranges from 2.59% for the 2% cycle to a maximum of 3.97% for the first 6% strain cycle. This is considerably less than what was observed for the wire. This is a result of the decreased hysteresis, which resulted in less energy dissipation. Overall, the 25.4 mm (1.0 in.) bar exhibited good superelastic behavior, as measured by its ability to have a small residual deformation following cycling to 6% strain. The most significant difference between the wire and bars is in the equivalent viscous damping ratio.

Comparison of Shape Memory Alloy Wire and Bars

The previous section showed the stress–strain behavior for 1.8 mm (0.071 in.) wire, and 25.4 mm (1.0 in.) diameter bar. For each sample size, a number of cyclic loading tests (6–10) were performed under the same loading conditions to confirm the behavior and ensure consistency within a sample set. The cyclic stress–strain response within each set was similar. This is expected, since in each case the samples were obtained by subdividing a larger segment. In addition, the samples within a set were heat treated and tested under the same conditions. While the behavior within a set was similar, differences in the cyclic stress–strain behavior were observed between the wires and bars. In particular, the load-

ing plateau, unloading plateau, and equivalent viscous damping of the wires and bars showed some moderate differences. Results from 7.1 mm (0.28 in.) and 12.7 mm (0.5 in.) diameter bars also show different characteristics from the wires and 25.4 mm (1.0 in.) diameter bars. Fig. 5 shows a comparison of the typical stress–strain behavior for the first 6% cycle for the four sets of samples. As shown in the plot, there are substantial differences between the stress–strain plots of the wire and bar samples. The SMA wires have the highest loading stress and the lowest unloading stress, which results in a higher equivalent viscous damping than the bars. The 12.7 mm (0.50 in.) diameter bars have the most significant strain hardening, which results in larger stresses at 6% strain than the other samples, but have the lowest equivalent viscous damping of all the samples. In general, the behavior of the

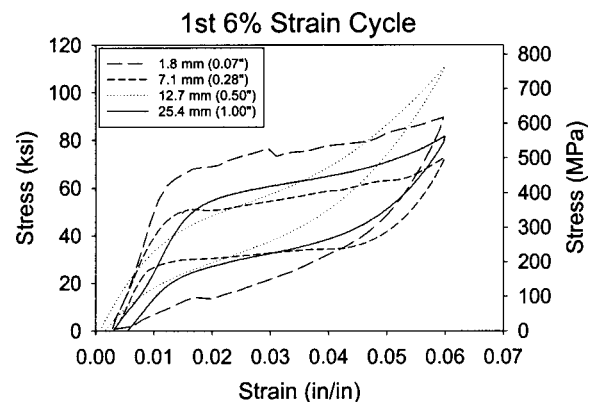


Fig. 5. Comparison of stress–strain curve for first 6% strain cycle for 1.8, 7.1, 12.7, and 25.4 mm diameter nitinol shape memory alloy wire and bars

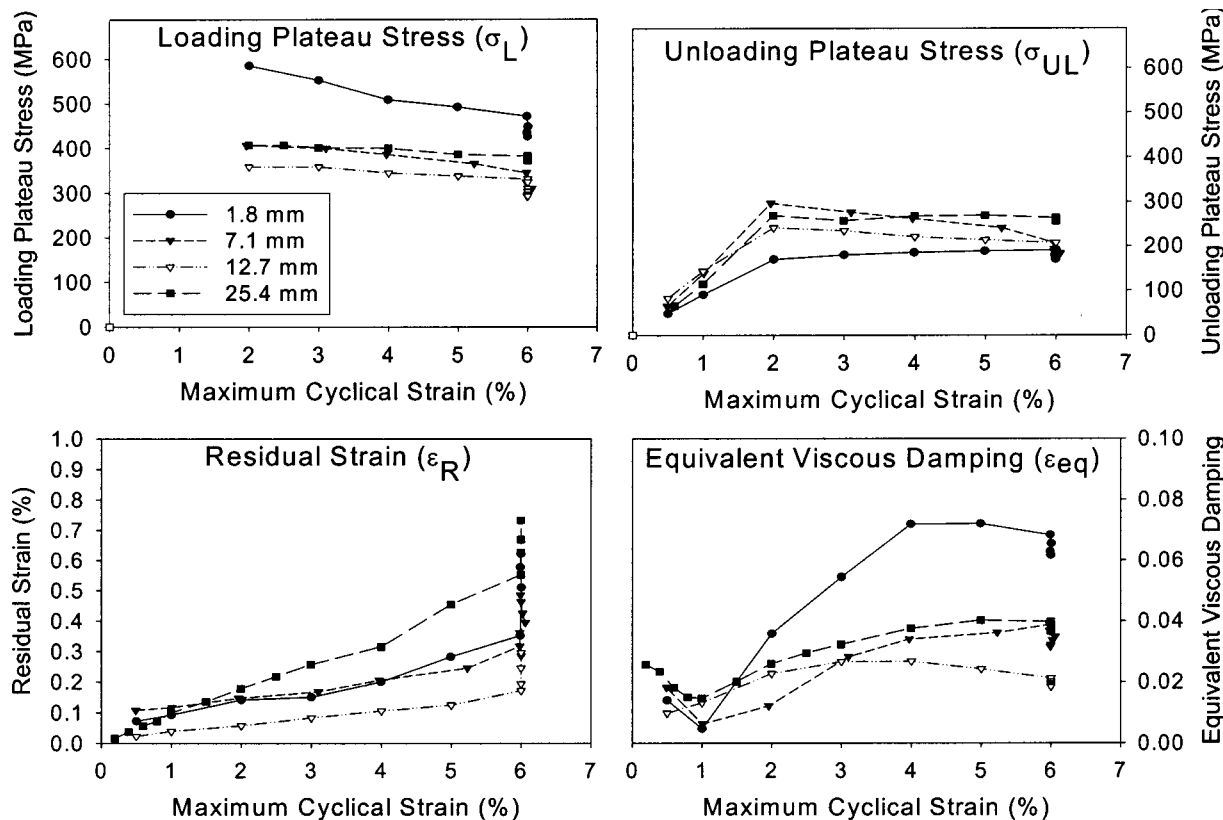


Fig. 6. Comparison of shape memory alloy wire and bars subjected to quasistatic cyclic loading showing: (a) loading stress plateau, σ_L , (b) unloading stress plateau, σ_{UL} , (c) residual strain, ε_r , and (d) equivalent viscous damping ratio, ξ_{eq}

7.1 mm (0.50 in.) and 25.4 mm (1.0 in.) diameter bars were similar in terms of loading and unloading stress and energy dissipation. The most interesting, and perhaps most important finding for applications of seismic resistant design is that both wire and bar samples exhibited very good recentering capability, refuting earlier studies that suggests that superelastic properties in large diameter bars are difficult to achieve. In all cases, the residual strains are less than 0.75% after the bars have been subjected to 6% cyclic strains.

Fig. 5 underscores one of the major concerns with shape memory alloys. The mechanical characteristics of the material are extremely sensitive to the composition and thermo-mechanical heat treatment provided to the material. Previous studies have shown that a 0.10% difference in the amount of titanium can significantly affect the loading plateau stress and the overall shape of the stress-strain hysteresis (Serneels 1999). This effect would have to be better understood and quality control would need to be enforced before shape memory alloys can be widely used in civil engineering applications. To better understand and quantify the differences between the various samples, the mechanical properties of SMAs are evaluated as a function of cyclic strain and bar diameter.

Comparison of Cyclic Properties of Shape Memory Alloys

Fig. 6 shows the loading plateau stress, σ_L , unloading plateau stress, σ_{UL} , residual strain, ε_r , and equivalent viscous damping, ξ_{eq} , as a function of the cyclic strain for the SMA wire and bar

samples. In all cases, the mean responses from each set are shown. As shown in the Fig. 6(a), the wire samples have considerably higher strength compared with the SMA bar samples. The differences are due to a combination of slightly different compositions and differences in the thermo-mechanical processing. Previous studies have shown that cold working increases the strength of superelastic shape memory alloys (Serneels 1999). The other major observation is that the loading plateau stress slightly decreases for successive cyclic loads for both the wire and bar samples. The decrease in the loading stress from the 2% cycle to the first cycle at 6% is approximately 130 MPa (18.9 ksi) for the wire sample. Much smaller reductions were observed for the SMA bar samples. As previously mentioned, the decrease in the loading stress is a result of localized slip, which facilitates the formation of stress-induced martensite. This behavior has been shown to decrease and stabilize for a large number of cycles (Mizayaki et al. 1986). Given this stabilization behavior, many have recommended “training” or preloading superelastic SMAs to limit the fatigue effect in shape memory alloys (MANSIDE 1998; Miyazaki et al. 1986).

Fig. 6(b) shows the unloading plateau stress values for the wire and bar samples as a function of loading strain. The figure shows that the unloading plateau stress increases during the low strain ranges, up to 2% strain. With the exception of the 1.8 mm (0.071 in.) diameter wires and 25.4 mm (1.0 in.) diameter bars, subsequent loading beyond 2% strain leads to slight decreases in the unloading plateau. Overall, the reduction in the unloading plateau is much less than the reduction in the loading plateau stress, which leads to a narrowing of the hysteresis, and therefore less energy dissipation.

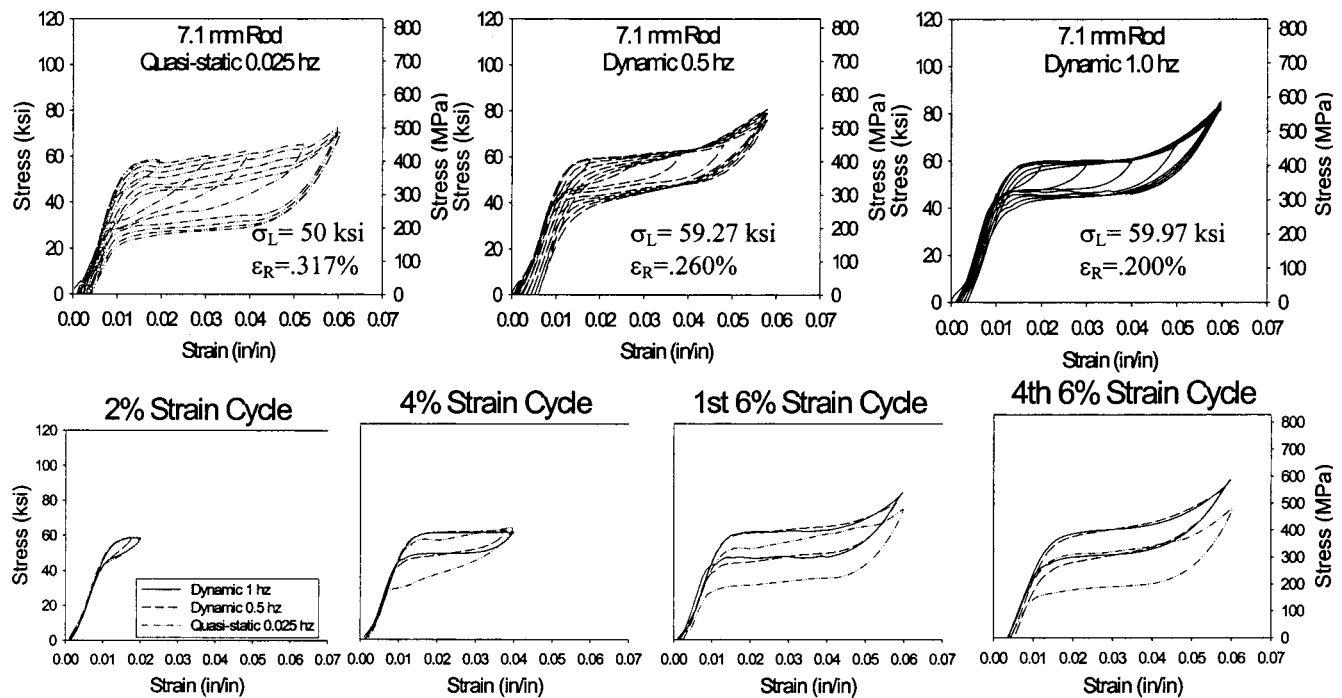


Fig. 7. Comparison of static and dynamic loading on 7.1 mm diameter shape memory alloy bar

Fig. 6(c) shows that for both the wires and bars, the residual strain increases, as the cyclic strain increases. That effect has been previously observed for SMA wires and is also a result of localized slip during stress-induced martensitic transformation. The residual strain after the first 6% cycle is largest for the 25.4 mm (1.0 in.) diameter bars $-\epsilon_r=0.55\%$, and smallest for the 12.7 mm (0.5 in.) diameter bars $-\epsilon_r=0.17\%$. There is no clear relationship between bar size and residual strain. Successive cyclic loading at 6% strain results in slight increases in residual strain. After completing four cycles at 6%, the residual in the 25.4 mm (1.0 in.) diameter bar increases from 0.55 to 0.73%. In general, the results show that both the superelastic wires and large bars exhibit good superelastic behavior for the range of cyclic strains up to 6%.

Fig. 6(d) shows the equivalent viscous damping for the superelastic wires and bars as a function of the cyclic strain. Several important observations can be made. First, the equivalent viscous damping typically reaches a maximum at approximately 4–5% strain and begins to decrease. This result can be easily understood by examining a typical stress–strain plot for the wire or 25.4 mm diameter bar, as shown in Figs. 3 and 4. For cyclical strains up to 5%, the area enclosed by the stress–strain curve increases rapidly due to the increase in strain, but more importantly due to the decrease in the reverse transformation stress. The unloading stress, σ_{UL} , decreases for increasing strains up to approximately 5% strain, after which the behavior stabilizes. This results in increasing equivalent viscous damping ratios for increasing strains. Beyond 5% strain, the SMA wire and bars begin to experience strain hardening. The strain hardening, coupled with the slight decrease in forward transformation results in slight reductions in the equivalent viscous damping. The equivalent viscous damping ranges from a maximum of 6.8% for the wires to a minimum of 2.1% for the 12.7 mm (0.5 in.) diameter bars, based on the first 6% strain cycle. In general, the bars have much lower equivalent viscous damping compared with the superelastic wire.

While the superelastic shape memory alloys exhibit hysteresis, the energy dissipation resulting from the hysteretic behavior is generally too low for the superelastic SMAs to be used in purely damping applications. The martensitic form of superelastic SMAs has shown significantly higher damping potential, with equivalent viscous damping typically on the order of 20–25% (MANSIDE 1998; Delemont 2002). However, the recentering capability of superelastic SMAs, coupled with the moderate damping, may result in superior performance in earthquake engineering applications, compared with the martensitic form of shape memory alloys. Moreover, it may be best to use a combination of superelastic and martensitic shape memory alloys to exploit the characteristics of both damping and recentering.

Effect of Dynamic Loading

Since the focus of this study is to evaluate the properties of superelastic SMAs for seismic applications, it is important to examine the effect of loading rate on the properties of the superelastic wire and bars. Previous studies of the strain rate effects on the properties of SMA wires have led to conflicting conclusions. Toubushi et al. (1998) showed that as the strain rate increased above 0.16%/s, the energy dissipated increased, compared with statically loaded SMAs. However, Wolons et al. (1998) found that at low frequencies, the dissipated energy may initially increase, but as the frequency increased above 0.1 Hz (1.0%/s), the energy dissipated becomes as small as 50% of the low frequency energy dissipation. Similar results to Wolons were observed by Dolce and Cardone (2001a,b). To determine the effect of loading rate, the cyclical tests are repeated at 0.5 Hz (6.0%/s) and 1.0 Hz (12.0%/s). Fig. 7 shows the stress–strain plot for the 7.1 mm (0.28 in.) diameter superelastic bar tested at 0.025, 0.5, and 1.0 Hz. The results show that increases in strain rate lead to an increase in both the loading stress, σ_L , and the unloading stress,

σ_{UL} . The loading stress for the first 6% strain cycle increases from $\sigma_L = 345$ MPa (50 ksi) for the static loading, to $\sigma_L = 407$ MPa (59 ksi) for the 0.50 and 1.0 Hz loading frequencies. Larger increases were observed for the unloading stress, σ_{UL} . This resulted in a narrowing of the hysteresis and an overall reduction in the energy dissipated for the dynamic loading compared with the static loading. The equivalent viscous damping for the first 6% strain cycle decreased from 3.87% during static loading to 2.39 and 1.82% during the 0.5 and 1.0 Hz loading frequencies, respectively. The increases in the loading and unloading stress are a result of an increase in temperature in the specimen during cycling. The heat of transformation results in self heating of the specimen during testing. As previously noted, the martensitic transformation is thermo-mechanical, meaning that an increase in temperature is equivalent to a decrease in stress. Therefore, as the temperature increases, there is an equivalent decrease in stress, resulting in a requirement of larger stress to induce martensite.

The recentering capability, measured from the residual strain, is shown to be insensitive to the strain rate. The residual strain under static loading (0.025 Hz) after the first 6% strain cycle is approximately the same as under dynamic loading. Similar observations were made for a set of 1.8 mm (0.071 in.) diameter wire, and 12.7 mm (0.50 in.) and 25.4 mm (1.0 in.) diameter bars.

Conclusions

This study involved the testing of superelastic SMA wires and bars to determine the cyclic properties and potential of SMAs, in particular those with large cross sections, in seismic resistant design and retrofit applications. The effects of loading history, loading frequency and bar size on the mechanical properties such as “yield” stress, damping, and recentering provide a valuable guide in determining the appropriate use of superelastic shape memory alloys in seismic applications.

In general, both the wire and bar form of the material show very good superelastic behavior. The residual strain gradually increases from an average of 0.15% following 3% strain to an average of 0.65% strain following four cycles at 6% strain. The residual strain does not appear to be a function of the bar diameter, with the 12.7 mm (0.5 in.) diameter bars showing the smallest residual strain of the four sets of samples. Continued loading beyond 6% strain typically resulted in unacceptably large increases in residual strains.

The forward transformation stress, typically referred to as loading stress plateau, σ_L , ranges from approximately 350 to 550 MPa (50.8–79.8 ksi). Cyclic loading of the SMA wire and bars led to slight reductions in loading stress plateau due to the fatigue effect. Fatigue results from small levels of localized slip that assist the forward transformation, which results in lower values of the loading stress plateau, σ_L .

An important property of SMAs for application in seismic resistant design and retrofit is damping. Equivalent viscous damping is computed for the SMA wire and bars as a function of the cyclic strain level. The equivalent viscous damping reached a maximum at approximately 4–5% strain and began to decrease for strains beyond 5%. The decrease is primarily due to the reduction in loading stress plateau, σ_L , and the strain hardening that occurs for larger strains. More importantly, the equivalent viscous damping is generally low—ranging from 2.0% for the 12.7 mm (0.5 in.) bar to a maximum of 7.6% for the 1.8 mm (0.071 in.) wires. These values are generally too low for consid-

eration of superelastic SMAs in purely damping applications. However, when combined with the recentering capability, the properties may be well suited for seismic applications. In addition, for supplemental damping, SMAs in martensitic form can be used in combination with superelastic SMAs as they have been shown to have significant damping characteristics.

Rate effects are evaluated by testing the SMA wire and bars at loading frequencies of 0.025, 0.5, and 1.0 Hz. The results show that increased frequency leads to an increase in the loading and unloading plateau stresses, a reduction of the hysteresis, and a marked decrease in the equivalent viscous damping in the wire and bars. However, the recentering capability, measured by the residual strain, is not affected by loading rate.

The goal of this study was to illustrate the potential of SMAs in seismic application, with focus on the properties of the larger sections. While the study illustrated that similar mechanical properties of SMAs can be achieved in both wire and bars, careful consideration of other factors must be taken into account when determining whether to use the wire or bar for SMAs. The cost for producing large diameter bars are generally more compared with wire form, primarily due to low volume of production for large bars. In addition, the use of large diameter bars typically requires threading the SMAs, which is very difficult and expensive due to the hardness of the material.

The use of SMAs in structural and seismic applications is still in its early stage of research. However, the past few years have shown significant promise due to a decrease in price and improvement in material quality. While the price of shape memory alloys is still considered high compared with other civil engineering materials, the cost has reduced dramatically. The cost is expected to continue to decrease as production procedures are improved and as more applications warranting large sections are sought.

Acknowledgments

This study has been supported primarily by the CAREER Program of the National Science Foundation under Grant No. 0093868. Additional support was provided by the Transportation Research Board through the IDEA Program. The writers wish to thank Dr. Subhash Gupta and Mr. Frank Sczerzenie of Special Metals Corporation who provided the material used in this study and advice on the thermo-mechanical heat treatment.

Notation

The following symbols are used in this paper:

- A_f = austenite finish temperature;
- A_s = austenite start temperature;
- E_i = initial modulus of elasticity;
- M_d = maximum temperature at which martensite occurs;
- M_f = martensite finish temperature;
- M_s = martensite start temperature;
- ε_r = residual strain;
- ξ_{eq} = equivalent viscous damping ratio;
- σ_L = loading plateau stress; and
- σ_{UL} = unloading plateau stress.

References

- Adachi, Y., and Unjoh, S. (1999). “Development of shape memory alloy damper for intelligent bridge systems.” *Proc. SPIE*, 3671, 31–42.

- Asai, M., and Suzuk, Y. (2000). "Applications of shape memory alloys in Japan." *Mater. Sci. Forum*, 327–328, 17–22.
- Beauchamp, C. H. (1992). "Shape memory alloy adjustable camber (SMAAC) control surfaces." *Proc., 1st European Conf. on Smart Structures and Materials*, Glasgow, U.K., 189–192.
- Chandra, R. (2001). "Active shape control of composite blades using shape memory actuation." *Smart Mater. Struct.*, 10, 1018–1024.
- Clark, P., Aiken, I., Kelly, J., Higashino, M., and Krumme, R. (1995). "Experimental and analytical studies of shape memory alloy dampers for structural control." *Proc., Passive Damping*, San Diego.
- Delemont (2002). "Seismic retrofit of bridges using shape memory alloys." Masters thesis, Georgia Institute of Technology, Atlanta.
- Dolce, M., and Cardone, D. (2001a). "Mechanical behaviour of shape memory alloys for seismic applications 1. Martensite and austenite NiTi bars subjected to torsion." *Int. J. Mech. Sci.*, 43(11), 2631–2656.
- Dolce, M., and Cardone, D. (2001b). "Mechanical behaviour of shape memory alloys for seismic applications 2. Austenite NiTi wires subjected to tension." *Int. J. Mech. Sci.*, 43(11), 2657–2677.
- Dolce, M., and Marnetto, R. (1999). "Seismic devices based on shape memory alloys." *Manside Project, III105-134*. Italian Dept. for National Technical Services, Rome.
- Duerig, T., Melton, K., Stokel, D., and Wayman, C. (1990). *Engineering aspects of shape memory alloys*, Butterworth–Heinemann, London.
- Friend, C. M., and Morgan, N. (1999). "Fatigue/cyclic stability of shape-memory alloys." *SMST-99: Proc., 1st European Conf. on Shape Memory and Superelasticity*, Atwerp Zoo, Belgium, 115–128.
- Graesser, E., and Cozzarelli, F. (1991). "Shape-memory alloys as new materials for aseismic isolation." *J. Eng. Mech.*, 117(11), 2590–2608.
- Hsu, S. E., Yeh, M. T., Hsu, I. C., Chang, S. K., Dai, Y. C., and Wang, J. Y. (2000). "Pseudo-elasticity and shape memory effect on the TiNi-CoV alloy." *Mater. Sci. Forum*, 327–328, 119–122.
- Inaudi, J., and Kelly, J. (1994). "Experiments on tuned mass dampers using viscoelastic, frictional and shape-memory alloy materials." *Proc., 1st World Conf. on Structural Control*, Los Angeles, 127–136.
- Kawaguchi, M., Ohashi, Y., and Tobushi, H. (1991). "Cyclic characteristics of pseudoelasticity of Ti–Ni alloys (effect of maximum strain, test temperature and shape memory processing temperature)." *JSME Int. J.*, 34(1), 76–82.
- MANSIDE. (1998). "Memory Alloys For New Structural Vibrations Isolating Devices." *Manside Third Twelve Monthly Progress Rep.*, Italian Dept. for National Technical Services, Rome.
- Miyazaki, S. (1990). *Thermal and stress cycling effects and fatigue properties of Ni–Ti alloys, engineering aspects of shape memory alloys*, T. W. Duerig, K. N. Melton, D. Stockel, and C. M. Wayman, eds., Butterworth–Heinemann, London, 394–413.
- Miyazaki, S., Imai, T., Igo, Y., and Otsuka, K. (1986). "Effect of cyclic deformation on the pseudoelasticity characteristics of Ti–Ni alloys." *Metall. Trans. A*, 17A, 115–120.
- Ocel, J., Leon, R. T., DesRoches, R., Krumme, R., Hayes, J., and Sweeney, S. (2002). "High damping steel beam-column connections using shape memory alloys." *Proc., 7th U.S. National Conf. in Earthquake Engineering*, Boston.
- Ohi, K. (2001). "Pseudo-dynamic earthquake response tests and cyclic loading tests on steel frames including pseudo-elastic elements." *Proc., NSF–JSPS, U.S.–Japan Seminar on Advanced Stability and Seismicity Concepts for Performance-Based Design of Steel and Composite Structures*, Kyoto, Japan.
- Serneels, A. (1999). "Shape memory alloy characterization and optimizations." *SMST-99: Proc., 1st European Conf. on Shape Memory and Superelasticity*, Atwerp Zoo, Belgium, 6–23.
- Strandel, B., Ohashi, S., Ohtsuka, H., Ishihara, T., and Miyazaki, S. (1995a). "Cyclic stress–strain characteristics of Ti–Ni and Ti–Ni–Cu shape memory alloys." *Mater. Sci. Eng., A*, 202, 148–156.
- Strandel, B., Ohashi, S., Ohtsuka, H., Miyazaki, S., and Ishihara, T. (1995b). "Effects of mechanical cycling on the pseudoelasticity characteristics of Ti–Ni and Ti–Ni–Cu alloys." *Mater. Sci. Eng., A*, 203, 187–196.
- Sweeney, S., and Hayes, J. (1995). "Shape memory alloy dampers for seismic rehabilitation of existing buildings." *Proc., 27th Joint Meeting on Wind and Seismic Effects, U.S.–Japan Cooperative Program in Natural Resources*, Tsukuba, Japan, 317–332.
- Tobushi, H., Iwanaga, H., Tanaka, H., Tatsuya, H., and Sawada, T. (1992). "Stress–strain–temperature relationships of TiNi shape memory alloy suitable for thermomechanical cycling." *JSME Int. J.*, 35(3), 271–277.
- Tobushi, H., Shimeno, Y., Hachisuka, T., and Tanaka, K. (1998). "Influence of strain rate on superelastic properties of TiNi shape memory alloys." *Mech. Mater.*, 30, 141–150.
- Wilde, K., Gardoni, P., and Fujino, Y. (2000). "Base isolation system with shape memory alloy device for elevated highway bridges." *Eng. Struct.*, 22(3), 222–229.
- Wolons, D., Gandhi, F., and Malovrh, B. (1998). "Experimental investigation of the pseudoelastic hysteresis damping characteristics of shape memory alloy wires." *J. Intell. Mater. Syst. Struct.*, 9(2), 116–126.